

PEDOT-Au Nanocomposite Films for Electrochemical Sensing of Dopamine and Uric Acid

J. Mathiyarasu*, S. Senthilkumar, K. L. N. Phani, and V. Yegnaraman

Electrodics and Electrocatalysis Division, Central Electrochemical Research Institute, Karaikudi 630006, India

In this work, conducting polymer impregnated gold nanoparticles are synthesized through a sequence of chemical and electrochemical routes. The nanocomposite film is characterized using UV-vis, FTIR spectroscopy, and SEM techniques to study the formation of oxidized PEDOT and Au⁰. The advantages of these films are demonstrated for sensing biologically important compounds such as dopamine and uric acid in presence of excess ascorbic acid, one of the major interferants in the detection of DA and UA (mimicking the physiological conditions), with superior selectivity and sensitivity when compared to the polymer film alone. Simultaneous determination is realized at 115 mV and 246 mV for DA and UA, respectively. The PEDOT matrix is recognized to be responsible for the peak separation (selectivity) while also favouring catalytic oxidation of the above compounds and the nanometer-sized gold particles allow nanomolar sensing of DA and UA (sensitivity). Thus, it is possible to detect nanomolar levels of DA and UA in presence of excess of AA. The combined effect of Au nanoparticles and the PEDOT matrix is rationalized that the Au_{nano} surrounded by a “hydrophobic sheath (PEDOT)” tending to reside within these hydrophobic regions of PEDOT, thus favouring the selectivity and sensitivity of the DA/UA detection. This new generation of nanocomposites is expected to enhance the value of electroanalytical techniques, as it is possible to tune their properties suiting the analytical needs.

Keywords: PEDOT, Gold, Nanocomposites, Sensor, Dopamine.

1. INTRODUCTION

Conducting polymers having conjugation system with in their backbone have received a great deal of attention because of their unique properties that suits for electrochemical applications.¹ Their tremendous commercial potential has touched off an outbreak of research, particularly on sensor devices, organic light-emitting diodes, transistors, solar cells, and memory devices.^{2–8} Conducting polymer incorporated with metallic or semiconducting nanoparticles provides an exciting system and the polymer-nanoparticles assembly holds great potential application in electronics, sensors, and catalysis.^{9–14} These composites have synergistic chemical and physical properties based on the constituent polymer and introduced metal. By tuning the polymer backbone with nanoscale materials, realization of nano-electronic sensor devices with superior performance is possible.

Sensors fabrication based on nanoparticle-incorporated polymeric matrices are of recent technological interest.^{15–16} Metal nanoparticles (Au, Ag, Pt) can be grown inside the polymer matrix by simultaneous electrodeposition of

polymer along with metal nanoparticles. Arrays of Au nanoparticles have been utilized for electrochemical sensors as they exhibit excellent catalytic activity towards various reactions.^{17–18} In these, the Au nanoparticles function efficiently as “electron antennae” and efficiently funneling electrons between the electrode/polymer interface and the electrolyte.¹⁹

Poly(3,4-ethylenedioxythiophene) (PEDOT) is an electrically conductive polymer with excellent long-term stability and relatively high transparency. In our earlier communications, we have demonstrated PEDOT polymer as a material of sensing matrix to detect biologically important molecules such as dopamine, ascorbic acid, and uric acid.^{20–22}

In this work, we take a leap forward, using Au nanoparticles incorporated PEDOT film as the sensing matrix by demonstrating the sensitivity at nanomolar levels. This is a one-component system where the polymer matrix offers the *selectivity* from the complex environment and the nanoparticles offer the required *sensitivity*, which is lacking in the polymer matrix alone. The sensitivity of the nanocomposite film was demonstrated in detecting the biomolecules such as dopamine and uric acid at nanomolar levels.

*Author to whom correspondence should be addressed.

2. EXPERIMENTAL DETAILS

2.1. Materials

All chemicals were obtained from Sigma-Aldrich, E-Merck, or Acros and used without further purification. The aqueous solutions were prepared using Milli-Q water (18.3 Ω) (Millipore).

2.2. Methods

For voltammetric studies, a glassy carbon (ϕ 3 mm, BAS, Inc.) working electrode, a platinum wire coil auxiliary electrode and an Ag|AgCl (3 M NaCl) reference electrode were used and the potential values mentioned in this text are referred to this reference electrode unless otherwise mentioned. A phosphate (0.1 M) buffer solution (PBS) of pH: 7.4 were employed as the electrolytic medium in electroanalysis experiment.

Electrochemical experiments were carried out using a Potentiostat/Galvanostat Autolab PGSTAT-30 (Eco-Chemie B.V., The Netherlands) at ambient temperature (25 ± 1 °C). To record the differential pulse voltammograms (DPV), the following input parameters were used: scan rate: 30 mV s⁻¹, sample-width: 17 ms, pulse-amplitude: 50 mV, pulse-width (modulation time): 50 ms, pulse-period (interval): 200 ms, and quiet-time: 2 s. Peak currents were determined by subtraction of a manually added baseline.

2.3. Instrumentation

TEM measurements were made using a Philips CM 200 machine and samples are handles using 400-mesh ultra thin carbon type-A copper grid. UV-vis spectrophotometry was performed using a UV-2401 (PL Shimadzu Spectrophotometer) and infrared spectroscopic measurements made using a Nexus FT-IR spectrometer 670 Model with DTGS detector. SEM measurements were made using Hitachi SEM (Field emission type). Model S 4700 with an acceleration voltage of 10 kV. The approximate film composition (± 2 atomic%) was analysed with an energy-dispersive fluorescent X-ray analysis (XRF-EDX) (Horiba X-ray analytical microscope XGT-2700).

3. RESULTS AND DISCUSSION

3.1. Synthesis of Au Nanoparticles

Au nanoparticles are prepared based on the biphasic procedure of Brust et al.²³ The Au nanoparticles are protected by monomer of EDOT by self-assembly of thiophene rings on gold surfaces.²⁴ An aqueous solution of hydrogen tetrachloroaurate (0.5 mM) was added to a solution of tetra *n*-octylammonium bromide (TOABr) in toluene (25 ml, 40 mM). The organic layer was separated out after the phase transfer of AuCl₄⁻. EDOT (10 mM) in toluene was

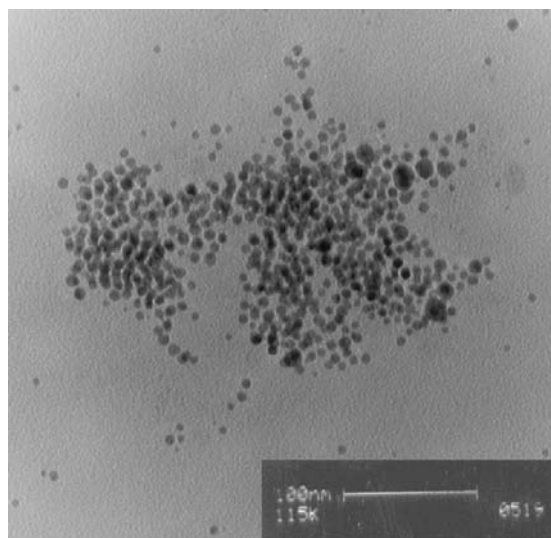


Fig. 1. TEM micrograph of EDOT protected Au nanoparticles.

added to this organic phase and the mixture was stirred for about 6 hours. A freshly prepared aqueous solution of sodium borohydride (20 ml, 10 mM) was added. A wine red colouration of the organic phase indicated the formation of Au nanoparticles surrounded/protected by EDOT. Toluene was evaporated using a rotary evaporator and the resulting residue was washed with acetone three times to remove the stabilizer (TOABr). Then, Au nanoparticles capped with EDOT was redissolved in acetonitrile. These particles are characterized by transmission electron microscopy which revealed (Fig. 1) that the particles are near-monodisperse around an average size of ~ 10 (± 0.1) nm, as calculated in a unit surface area (1.1 cm²) containing approximately 30 particles.

3.2. Preparation of Au-PEDOT Composite on Glassy Carbon Electrode Surface

Au_{nano}-PEDOT was electrochemically deposited as a continuous film on GCE from a solution of EDOT-protected AuNPs in acetonitrile containing tetrabutylammonium perchlorate as supporting electrolyte by potential scanning between -0.5 to 1.9 V versus Ag wire *pseudo*-reference electrode. Figure 2 shows that the current increases with successive potential scanning, indicating progress of electropolymerization of EDOT to PEDOT incorporating AuNPs. It is clear from the first voltammetric curve that a rapid growth of the anodic current density starts at ~ 1.40 V, which corresponds to the beginning of the EDOT monomer oxidation. The increase in anodic and cathodic peak current densities imply that the amount of polymer on the electrode surface increases. These cyclic voltammograms are quite similar to those reported for the electropolymerization of PEDOT in acetonitrile medium with other electrolytes.²⁵ The Au_{nano}-PEDOT composite film was allowed to grow on GCE surface for five successive

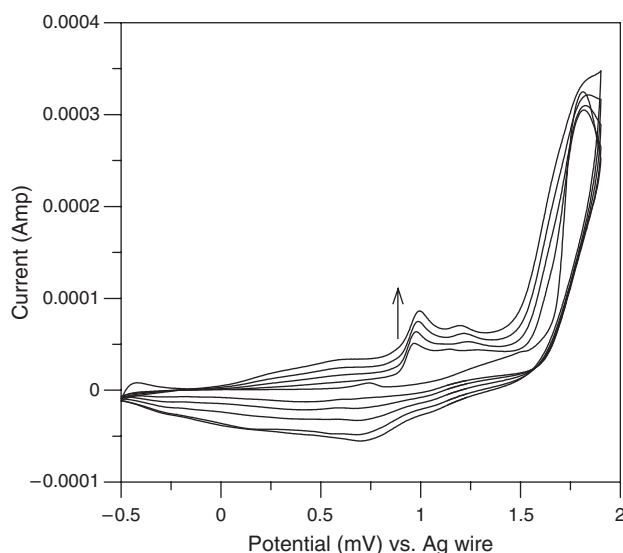


Fig. 2. Cyclic voltammogram of electro polymerized PEDOT-Au nanocomposite in 0.1 M TBAPC solution in acetonitrile. Sweep rate 0.1 V s⁻¹.

scans and the cycling was intentionally limited in order to obtain a thin film.

3.3. Characterization of Au_{nano}-PEDOT Composite

Figure 3, shows the absorption spectra of Au_{nano}-PEDOT composite film coated on ITO glass substrates.

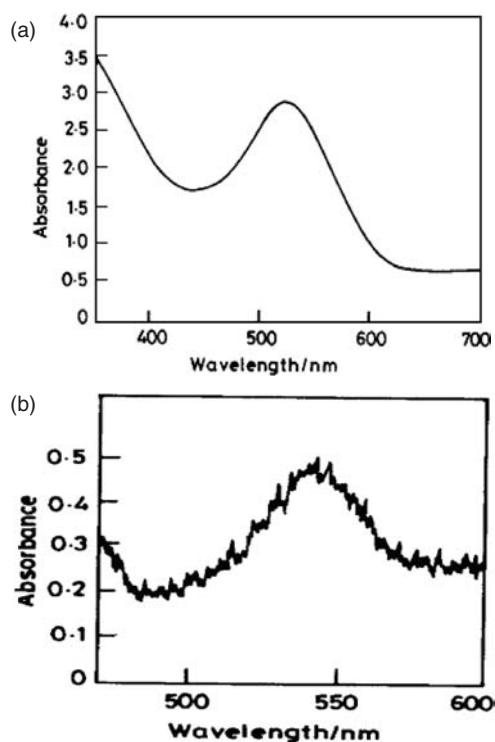


Fig. 3. UV-vis absorption spectra of (a) EDOT protected Au nanoparticles, (b) Au-nanoparticle incorporated PEDOT film.

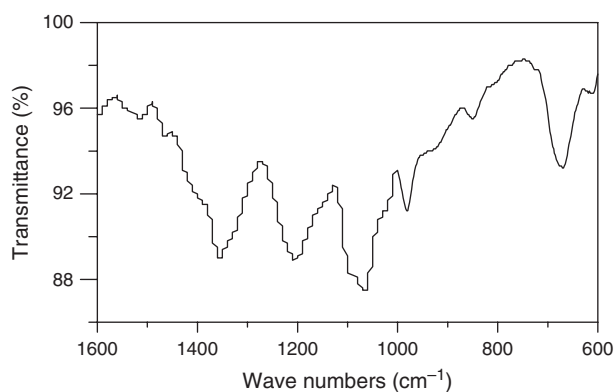


Fig. 4. FTIR spectra of Au_{nano}-PEDOT nanocomposite.

The spectrum obtained for the composite film is very similar to that of the EDOT protected Au nanoparticles, though the intensity is relatively small. Both Au in the solution and in the film give an absorption maximum at ~530 and 540 nm that corresponds to a particle size of ~10–20 nm.²⁶ XRF analysis of the Au_{nano}-PEDOT composite film also confirms the presence of Au nanoparticles (24%) along with sulphur (76%). A small red shift in the absorption values observed with the film is attributed to an increase in the cluster dimension due to the agglomeration of the particles during electropolymerization arising from the π - π interactions between the thiophene moieties.

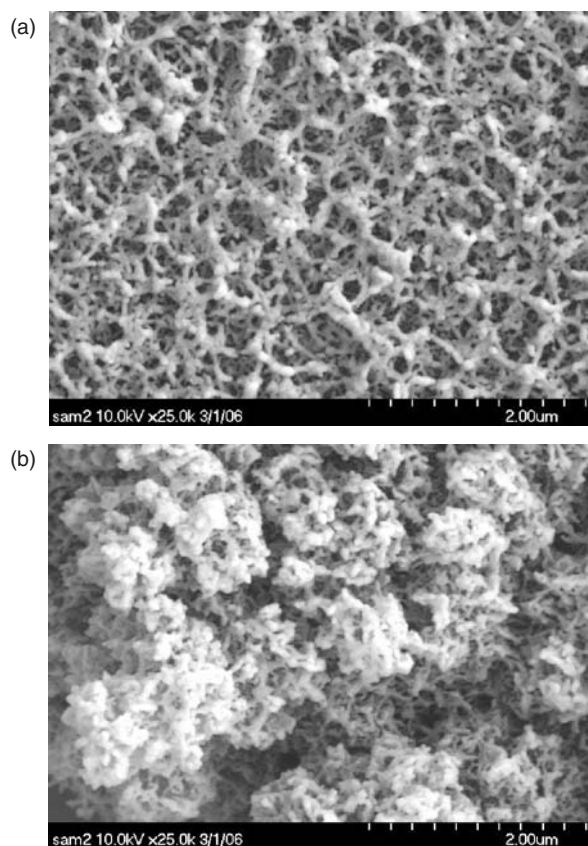
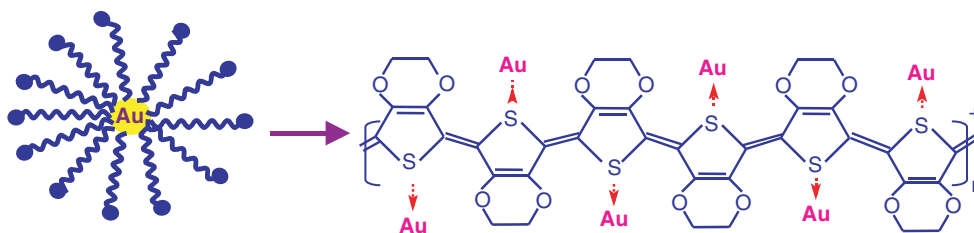


Fig. 5. SEM micrographs of (a) PEDOT and (b) Au_{nano}-PEDOT.



Scheme 1. Au_{nano} -PEDOT nanocomposite.

Figure 4 shows the vibrational spectrum of the Au_{nano} -PEDOT composite film coated on a ITO glass substrate. The vibrations at around 1336 and 1519 cm^{-1} are due to $-C-C-$ or $-C=C-$ stretching of quinoidal structure and due to ring stretching of thiophene ring, respectively. Vibrations at 1186 , 1139 , and 1080 cm^{-1} originate from $-C-O-C-$ bond stretching in the ethylenedioxy group. $-C-S-$ bond in the thiophene ring are also seen at 977 , 833 , and 682 cm^{-1} . The band at around 1330 cm^{-1} due to the quinoidal structure, indicates that PEDOT in its doped state.^{27–28} Further the band at 1202 is due to the PEDOT oxidized structure.²⁹

The FE-SEM images of the electropolymerised PEDOT film and Au_{nano} -PEDOT nano composite film coated on ITO glass substrates are shown in Figure 5. PEDOT alone shows fibrillar network structure with a fiber dimensions of $\sim 20\text{ nm}$. The polymer network with a highly porous structure can be seen, which might easily entrap Au nanoaggregates. The image of the PEDOT after incorporation of AuNPs shows that the structure and morphology of the

polymer film change significantly. As can be seen from Figure 5(b), the fibrils are coated with AuNP aggregates with high porosity indicating its possible application in producing high surface area materials. On independent examination using the voltammetric response of Au (figure not shown), the AuNPs were found to be very stably attached to the polymer nanofibrillar matrix.

3.4. Sensing Behavior of Au-PEDOT Composite

PEDOT is known to contain a distribution of hydrophobic (reduced) and hydrophilic (oxidized) regions.³⁰ We have earlier established this feature using current-sensing AFM.²⁰ On polymerization of EDOT, the Au_{nano} tend to reside within these “hydrophobic regions” of PEDOT (Scheme 1). Hydrophobic analytes such as dopamine interacts with these regions and the more hydrophilic ones prefer the oxidized regions of PEDOT. This behavior is favourable for selectivity and sensitivity in electroanalysis of molecules.

To demonstrate the utility of nanoparticles incorporation in the polymer film, electroanalysis of DA and UA in presence of excess of AA was performed using Au_{nano} -PEDOT nanocomposite film. Figure 6 exhibits the DPV's obtained for varying DA and UA concentrations in the presence of a fixed concentration of AA on Au_{nano} -PEDOT modified electrode. The voltammetric peak current of AA oxidation remains unchanged, whereas the oxidation current of DA and UA increases linearly as the bulk concentration of DA and UA is increased. In our earlier reports^{21–22} the detection limits of DA and AA on PEDOT modified GCE were found to be in the range of micro-molar concentrations. The Au_{nano} -PEDOT electrode shows better performance and the detection limit of DA/UA in the presence of 0.5 mM of AA was found to be $2 (\pm 0.05)\text{ nM}$. The calibration for DA and is found to be linear with a correlation coefficient (R^2) of 0.99 and 0.98 and with a slope value of 0.20 and $0.12\ \mu\text{A} \cdot \text{nM}^{-1}$ for dopamine and uric acid, respectively.

4. CONCLUSIONS

Au_{nano} -PEDOT nanocomposites were prepared successfully using chemical and electrochemical routes. The UV-vis and FTIR results confirmed incorporation of Au nanoparticles of $10\text{--}20\text{ nm}$ size with in the polymer matrix.

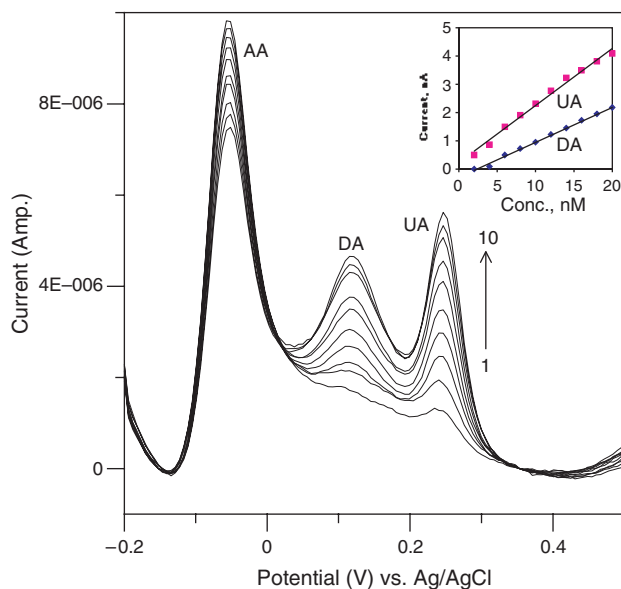


Fig. 6. Differential pulse voltammograms of Au-PEDOT coated electrode in phosphate buffer solution (pH 7.4) containing 0.5 mM AA with different concentrations of DA and UA. The numbers 1–10 correspond to mixed solutions of 2, 4, 6, 8, 10, 12, 14, 16, 18, and 20 nM . Inset shows plots of the peak currents as a function of concentration of (a) DA and (b) UA in the range of $2\text{--}20\text{ nM}$.

FE-SEM morphology reveals that the AuNPs were found to attach stably to the polymer nanofibrillar matrix. The combined effect of Au nanoparticles and the PEDOT matrix is rationalized that the Au_{nano} surrounded by a “hydrophobic sheath (PEDOT)” tending to reside within these hydrophobic regions of PEDOT. The advantages of these films are demonstrated for sensing biologically important compounds such as dopamine and uric acid in presence of excess ascorbic acid, one of the major interferants in the detection of DA and UA (mimicking the physiological conditions), with superior selectivity and sensitivity when compared to the polymer film alone.

Acknowledgments: One of the authors (J.M.) thanks the Department of Science & Technology, New Delhi for a research grant under SERC Fast Track Scheme No. SR/FTP/CS-35/2004.

References and Notes

1. T. A. Skotheim, R. L. Elsenhaumer, and J. R. Reynolds (ed.), *Handbook of Conducting Polymers*, 2nd edn., Marcel Dekker, New York (1999).
2. J. H. Burroughs, D. D. C. Bradley, A. R. Brown, R. N. Marks, K. Mackay, R. H. Friend, P. L. Burns, and A. B. Holmes, *Nature* 347, 539 (1990).
3. M. Leclerc, *Adv. Mater.* 11, 1491 (1999).
4. P. S. Heeger and A. J. Heeger, *Proc. Natl. Acad. Sci.* 96, 12219 (1999).
5. J. H. Burroughes, C. A. Jones, and R. H. Friend, *Nature* 335, 137 (1988).
6. M. R. Andersson, O. Thomas, W. Mammo, M. Svensson, M. Theander, and O. Inganäs, *J. Mater. Chem.* 9, 1933 (1999).
7. N. S. Sariciftci, L. Smilowitz, A. J. Heeger, and F. Wudl, *Science* 258, 1474 (1992).
8. G. Yu, J. Wang, L. McElvain, and A. J. Heeger, *Adv. Mater.* 10, 1431 (1998).
9. K. M. Kost, D. E. Bartak, B. Kazee, and T. Kuwana, *Anal. Chem.* 60, 2379 (1988).
10. A. Kitani, T. Akashi, K. Sugimoto, and S. Ito, *Synth. Met.* 121, 1301 (2001).
11. W.-H. Kao and T. Kuwana, *J. Am. Chem. Soc.* 106, 473 (1984).
12. F. Ficicioglu and F. Kadirgan, *J. Electroanal. Chem.* 430, 179 (1997).
13. A. Drelkiewicz, M. Hasik, and M. Kloc, *Catal. Lett.* 64, 41 (2000).
14. E. T. Kang, Y. P. Ting, K. G. Neoh, and K. L. Tan, *Synth. Met.* 69, 477 (1995).
15. C. R. Raj, T. Okajima, and T. Ohsaka, *J. Electroanal. Chem.* 543, 127 (2003).
16. R. Gangopadhyay and A. De, *Chem. Mater.* 12, 608 (2000).
17. A. Doron, E. Katz, and I. Willner, *Langmuir* 11, 1313 (1995).
18. A. N. Shipway, E. Katz, and I. Willner, *Chem. Phys. Chem.* 1, 18 (2000).
19. K. R. Brown, A. P. Fox, and M. J. Natan, *J. Am. Chem. Soc.* 118, 1154 (1996).
20. S. Senthil Kumar, J. Mathiyarasu, and K. L. N. Phani, *J. Electroanal. Chem.* 578, 95 (2005).
21. S. Senthil Kumar, J. Mathiyarasu, K. L. N. Phani, and V. Yegnarman, *J. Solid State Electrochem.* 10, 905 (2006).
22. S. Senthil Kumar, J. Mathiyarasu, K. L. N. Phani, Y. K. Jain, and V. Yegnarman, *Electroanalysis* 17, 2281 (2005).
23. M. Brust, M. Walkes, D. Bethell, D. J. Schiffrin, and R. Whyman, *J. Chem. Soc. Chem. Commun.* 801 (1994).
24. J. Noh, E. Ito, K. Nakajima, J. Kim, H. Lee, and M. Hara, *J. Phys. Chem. B* 106, 7139 (2002).
25. P.-H. Aubert, L. Groenendaal, F. Louwet, L. Lutsen, D. Vanderzande, and G. Zotti, *Synth. Met.* 126, 193 (2002).
26. K. R. Brown, D. G. Walter, and M. J. Natan, *Chem. Mater.* 12, 306 (2000).
27. M. Lapkowskis and A. Pron, *Synthetic Metals* 110, 79 (2000).
28. C. Kearnström, H. Neugebauer, S. Blomquist, H. J. Abonene, J. Kankare, and A. Ivaska, *Electrochim. Acta* 44, 2739 (1999).
29. W. W. Chiu, J. T. Sejdic, R. P. Cooney, and G. A. Bowmaker, *Synth. Met.* 155, 80 (2005).
30. C. R. Martin and L. S. Van Dyke, *Molecular Design of Electrode Surfaces*, edited by R. W. Murray, Wiley, New York (1992), pp. 403–424.

Received: 17 March 2006. Accepted: 31 August 2006.